



Chemical characterization of air pollution in Eastern China and the Eastern United States

Xuexi Tie^{a,b}, Guy P. Brasseur^{a,c}, ChunSheng Zhao^{d,*}, Claire Granier^{c,e,f},
Steven Massie^a, Yu Qin^d, PuCai Wang^b, Geli Wang^b,
PeiCai Yang^b, Andreas Richter^g

^aNational Center for Atmospheric Research, Boulder, CO USA

^bInstitute of Atmospheric Physics, Chinese Academy of Sciences, China

^cMax-Planck Institute of Meteorology, Hamburg, Germany

^dDepartment of Atmospheric Science, School of Physics, Peking University, Beijing 100871, China

^eAeronomy Laboratory, NOAA, Boulder, CO, USA

^fService d'aéronomie/IPSL, Paris, France

^gUniversity of Bremen, Bremen, Germany

Received 25 July 2005; received in revised form 29 November 2005; accepted 29 November 2005

Abstract

Satellite data (MODIS, GOME, and MOPITT) together with a chemical transport global model of the atmosphere (MOZART-2) are used to characterize air pollution in Eastern China and the Eastern US to assess the differences between the photochemical conditions in these two regions. Observations show that aerosol concentrations (both fine (radius < 0.5 μm) and coarse modes (radius > 0.5 μm)) are higher in Eastern China than in the Eastern US. The NO_x concentrations in both regions are substantially higher than in remote regions such as over the oceans (150 compared to 5 (10¹⁴ # cm⁻²) over the Pacific Ocean). The CO concentrations are high in both urbanized areas (30 compared to 10 (10¹⁷ # cm⁻²) over the Pacific Ocean). However, the concentrations of non-methane hydrocarbons from both anthropogenic and biogenic sources are considerably lower in Eastern China than in the Eastern US. As a result, the rate of photochemical ozone production and ozone concentrations during summer is significantly lower in Eastern China (daily averaged concentrations of 40–50 ppbv in summer) than in the Eastern US (daily averaged values of 60–70 ppbv). The analysis also shows that in Eastern China, the O₃ production is mainly due to the oxidation of carbon monoxide (54% of total O₃ production), while, in the Eastern US, the O₃ production is attributed primarily to the oxidation of reactive hydrocarbons (68% of total O₃ production). The results also indicate that biogenic emissions of hydrocarbons contribute substantially to the production of O₃ in the Eastern US. The O₃ production due to the oxidation of biogenic hydrocarbons represents approximately one third of total O₃ photochemical production in this region. Measurements of surface ozone in the Eastern US and Eastern China seem to support that the summer ozone production is lower in Eastern China than in the Eastern US. However, additional surface measurements, especially of reactive hydrocarbons and ozone are needed in Eastern China in order to improve the present analysis and to confirm our current conclusions. A sensitivity study shows

*Corresponding author. Tel.: +86 10 6275 4684; fax: +86 10 6275 1615.

E-mail address: zcs@pku.edu.cn (C. Zhao).

that with increase in anthropogenic emissions of HCs, the surface ozone concentrations significantly increase in Eastern China, indicating that the increase in the emissions of HCs plays an important role for the enhancement in surface ozone in this region.

© 2006 Elsevier Ltd. All rights reserved.

Keywords: Ozone production; The Eastern US; Eastern China

1. Introduction

Recent satellite observations (GOME-NO₂; SO₂, SCIAMACHY-NO₂, MOPITT-CO, MODIS-aerosols, etc.) have shown that there are very high air-pollution levels in Eastern China (high NO₂, CO, and aerosols) and in the Eastern US (high NO₂ and CO). These two regions are characterized by some similar conditions: (1) the two regions are located at mid-latitudes of the northern hemisphere (NH), (2) the two regions are in the Eastern parts of NH continents, and (3) both regions are populated areas with high industrial activity. However, the land cover is very different in the two areas: vegetation, which emits large quantities of biogenic hydrocarbons, is abundant in the Eastern US, while arid soils, which favor the mobilization of dust, are present in Eastern China. In addition, the type of fuel used for energy production is different in the two regions. For example, as stated by the International Energy Agency (IEA, 2004), the usage of coal during 2003 amounted to 1502 Tg (10¹² g in China and 976 Tg in the US, respectively). By contrast, the usage of crude oil was 234 Tg in China and 864 Tg in the US, respectively. Asian aerosol sources, unlike those in North America, originate from coal and biomass burning (Huebert et al., 2003). The extensive usage of coal is known to produce more SO₂ and aerosol pollution than oil fuel usage. The study by Sun et al. (2004) shows that coal burning and traffic exhaust, in addition to the dust originating from the Gobi desert, are major sources of aerosol pollution at Beijing, China. A report released in 1998 by the World Health Organization (WHO, 1998) noted that of the 10 most polluted cities in the world, 7 are found in China. Sulfur dioxide and soot produced by coal combustion are two major air pollutants, resulting in the formation of acid rain, which now affects about 30% of China's total land area. Industrial boilers and furnaces consume almost half of China's coal and represent the largest single sources of urban air pollution. In addition, economic expansion in China has unavoidably been accompanied by increases in

oil and gas burning. For example, the energy consumption in China has increased more than 300% from 1973 to 2002 (IEA, 2004).

In this paper, we use a chemical transport model simulations and satellite observations to analyze the chemical characterization of the Eastern China and the Eastern US. The comparison of the differences in chemical species, especially tropospheric ozone precursors and ozone productions, will provide information to better understand the chemical characterizations between the two regions. With a better knowledge of the current air pollution in Eastern China, we will be able to estimate the potential impact of future economical development on tropospheric ozone in Eastern China.

The paper is organized as follows. In Section 2, we briefly describe the tools (including satellite data and global model) used in the present study, and in Section 3, we present an analysis of the model simulations. Major conclusions are provided in Section 4.

2. Tools

In this Section, we present the satellite data and the global chemical transport model (MOZART-2) used in the present study. The satellite observations provide direct evidence for air pollution by gas-phase chemical compounds and aerosol particles, and can be used to evaluate the model calculations in the geographical areas under consideration. However, satellite data do not include information on the distributions of several chemical species that are needed to quantify the ozone budget. In this case, we use information provided by the MOZART-2 model. The model is also used to provide an estimate of the O₃ production resulting from specific oxidation processes.

2.1. Satellite data

There are several satellites that provide data sets on global scale air pollution, including global ozone monitoring experiment (GOME), measurements of

pollutants in the troposphere (MOPITT), and moderate resolution imaging spectroradiometer (MODIS). GOME measures NO₂ columns. The GOME spectrometer operates between 423 and 451 nm with a resolution of 0.29 nm, using a nadir scan with 40 × 320 km² footprint (Burrows et al., 1999). MOPITT is a thermal and near-IR nadir-viewing gas correlation radiometer (Drummond, 1992), that retrieves CO column, and CO mixing ratios vertical profiles with a spatial resolution of 22 × 22 km (Deeter et al., 2003). MODIS observes the Earth's surface in 36 spectral bands with horizontal resolutions between 250 m and 1 km. Optical depths are retrieved at 0.55 μm, and fine and coarse aerosol mode fractions are derived (Remer et al., 2002).

In the present study, we analyze GOME NO₂, MOPITT CO and MODIS aerosol optical depths. MOPITT CO columns, gridded at 1° latitude × 1° longitude are provided for the months of December–February and June–August. The MODIS retrievals of fine mode aerosols refer to the accumulation mode (radii less than 0.5 μm), while the coarse mode accounts for aerosol radii greater than 0.5 μm (Chu et al., 2003).

2.2. Global chemical transport model

MOZART-2 simulates the distribution of tropospheric ozone and its chemical precursors. In its standard configuration, the model calculates the concentrations of 63 chemical species from the surface up to the middle stratosphere. The model uses meteorological inputs derived either from a general circulation model or from a meteorological reanalysis. MOZART-2 is described in detail by Horowitz et al. (2003). This paper includes an extensive evaluation of MOZART-2, including a comparison of calculated concentrations with CMDL surface measurements (CO and O₃), global O₃ sonde observations, and measurements from aircraft (O₃, CO, NO_x, PAN, HNO₃, various HC, CH₂O, etc.). The horizontal resolution of the model and emission inventory is 2.8° in longitude and latitude.

The “standard” MOZART-2 model is developed within the framework of the transport model called model of atmospheric transport and chemistry (MATCH), developed by Rasch et al. (1997). It includes a representation of advection, convective transport, boundary layer mixing, and wet and dry deposition. Surface emissions of chemical species

include those from fossil fuel combustion and industrial activities, biomass burning, biological activity in vegetation and soils, and by the ocean. Aircraft emissions of NO_x and CO are provided according to the estimates by Friedl (1997). The chemical scheme used in MOZART-2 accounts for the oxidation of methane, ethane, propane, ethane, propene, isoprene, α-pinene (as a surrogate for all terpenes), and *n*-butane (as a surrogate for all hydrocarbons with 4 or more carbons, excluding isoprene and terpenes). Heterogeneous reactions of N₂O₅ and NO₃ on the surface of sulfate aerosols are included, using a prescribed sulfate aerosol distribution (Tie et al., 2001a).

The model has been applied in numerous scientific studies, including the analysis of data obtained from field campaigns and satellite observations and investigations of the impacts of physical and chemical processes on tropospheric oxidants and ozone distributions (see Brasseur et al. (1998), Hauglustaine et al. (1998), and Horowitz et al. (2003)). The impacts of biomass burning, NO_x production from lightning, and aerosols on tropospheric oxidants have also been investigated by Hauglustaine et al. (1999), Hauglustaine et al. (2001), and Tie et al. (2001a, b, 2002a, 2005). MOZART-2 has been used to study the ozone and NO_x budget over East Asia and over the US (Mauzerall et al., 2000; Zhang et al., 2003), to assess the effect of cloud droplets and biogenic methanol on the tropospheric oxidants (Tie et al., 2003b, c), and to analyze field campaign data and satellite observations, including TRACE-A, TRACE-P, TOPSE and MAPS (Cunnold et al., 2002; Lamarque and Hess, 2003; Lamarque et al., 1999; Tie et al., 2003a). The first version of MOZART was also used in a recent IPCC assessment (IPCC, 2001).

In this study, as model input, we use dynamical fields provided by the meteorological analysis of the European Center for Medium-range Weather Forecast (ECMWF). The MOZART-2 model is integrated from January 1996 to December 1997. The results obtained between January 1997 and December 1997 are used for this study.

2.3. Emissions in the two regions

The emissions are major factors that determine the distribution of primary chemical species, such as CO, NO_x, and HC etc. In order to characterize and compare the chemical composition in Eastern China

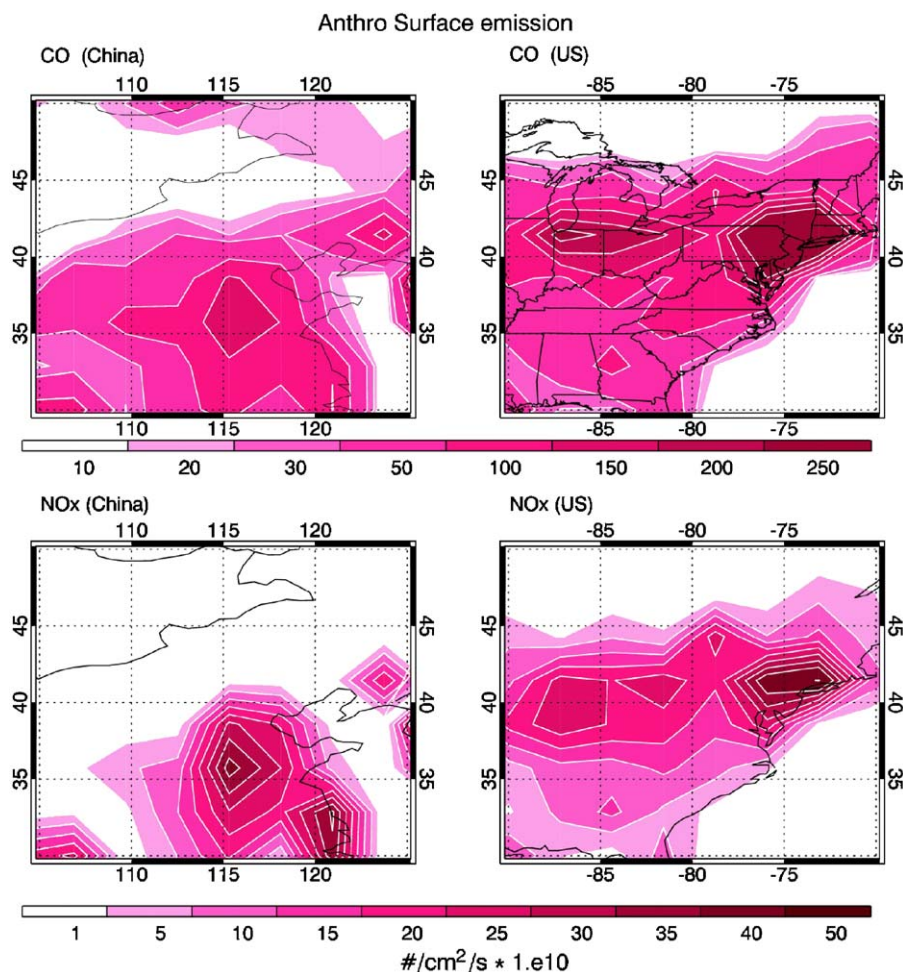


Fig. 1. Anthropogenic emissions of CO and NO_x ($10^{10} \# \text{cm}^{-2} \text{s}^{-1}$) in Eastern China (left panels) and in the Eastern US (right panels).

and the Eastern US, we first assess the chemical emissions in these two regions. Emissions are based on the global EDGAR v3.0 inventory for 1997 (Olivier et al., 2003). Fig. 1 shows the anthropogenic (fossil fuel) emissions of CO and NO_x in the two regions, Table 1 compares the global CO, NO, and HC emissions adopted in MOZART-2 with the estimations of Streets et al. (2003) for Eastern China. The annually averaged anthropogenic CO emissions (including fossil fuel, biofuel, and biomass burning) provided by EDGAR V3.0 are about 74 and 55Tg year^{-1} in Eastern China and in the Eastern US, respectively, while corresponding CO emissions estimated by Streets et al. (2003) for Eastern China are 58Tg year^{-1} . In the case of NO_x , the annually mean anthropogenic emissions are about 7.4 and 8.0Tg year^{-1} in Eastern China and in the Eastern US, respectively. The first of these values can be

Table 1
Emission characterization in Eastern China and in the Eastern US

	E. China (streets)	E. China (MOZ)	E. US (MOZ)
CO (Tg yr^{-1})	57.0	74.0	55.4
CO (fossil)		40.0	50.6
CO (biof + burn)		34.0	4.8
NO_x (Tg yr^{-1})	5.3	7.4	8.0
NO_x (fossil)		6.7	7.7
NO_x (biof + burn)		0.7	0.3
HCa (TgC yr^{-1})	8.3	8.1	13.6
HCb (TgC yr^{-1})		12.3	19.5

The CO and NO_x emissions include fossil fuel, biofuel, and biomass burning sources. The HCa is the anthropogenic source of hydrocarbon, and HCb is the biogenic emission of hydrocarbon.

compared to the 5.3 Tg year^{-1} estimated by Streets et al. (2003). In the case of hydrocarbons, the annually mean anthropogenic emissions are about 8.1 and $13.6 \text{ Tg year}^{-1}$ in Eastern China and in the Eastern US, respectively, compared to 8.3 Tg year^{-1} estimated by Streets et al. (2003) in the case of Eastern China. The estimated emissions for biogenic hydrocarbon (HCb) are 12.3 and $19.5 \text{ Tg year}^{-1}$ for Eastern China and the Eastern US, respectively. There is no estimate of biogenic emission by Streets et al. (2003). Overall, the anthropogenic hydrocarbon (HCa) used in MOZART-2 are comparable to the corresponding estimates by Streets et al. (2003). The estimated CO and NO_x emissions by MOZART-2 are somewhat higher than the estimates by Streets et al. (2003), primarily because larger biomass-burning emissions are adopted in the model.

Although, in both regions under consideration, the emissions of ozone precursors are very large, their origin is quite different. In Eastern China, the emissions are due largely to coal burning, while in the Eastern US, they are due mainly to automobile exhaust (Sun et al., 2004; IEA, 2004). Fig. 2 shows the emissions of biogenic hydrocarbons (labeled HCb and including isoprene and α -pinene as a surrogate for all terpenes) and the emissions of anthropogenic hydrocarbons (noted HCa and including ethane, propane, ethane, propene, and *n*-butane as a surrogate for all hydrocarbons with 4 or more carbons) in these two regions. It shows that the HCb and HCa emissions are considerably larger in the Eastern US than in Eastern China. The annually averaged HCa emission amounts to about 4.5 and $14.7 \text{ Tg C year}^{-1}$, and the HCb emission to about 12 and 20 Tg year^{-1} in Eastern

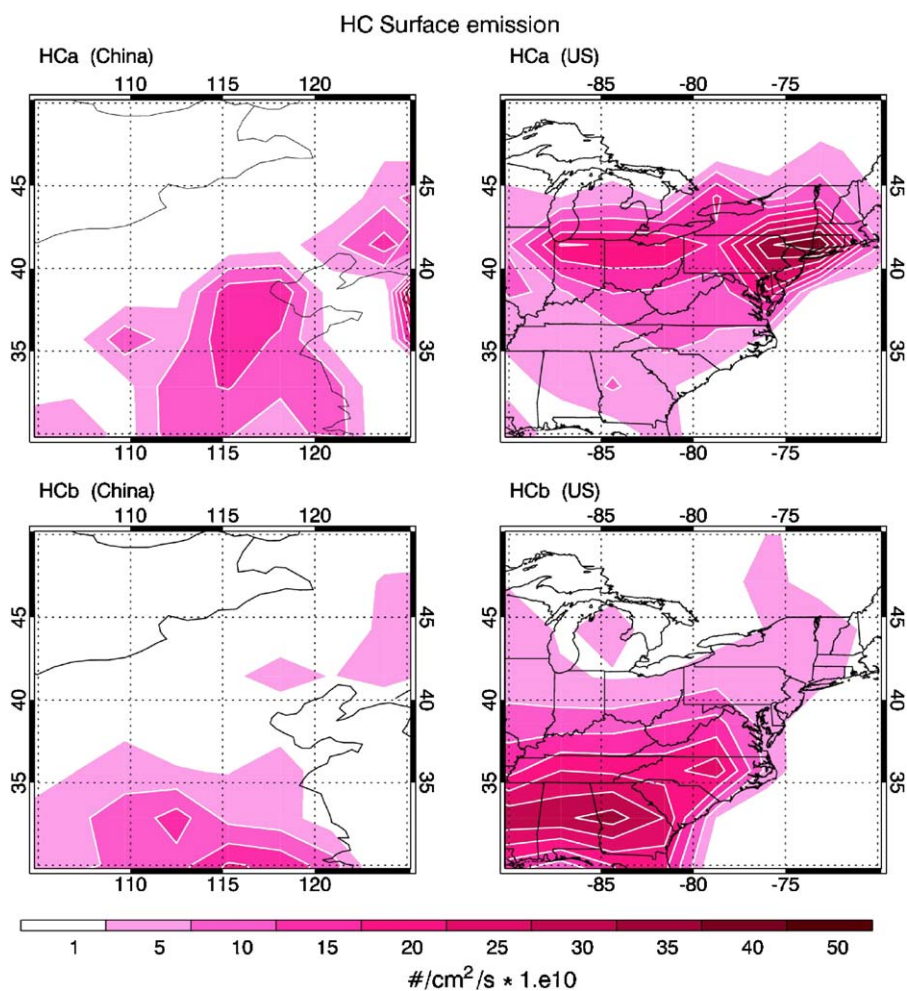


Fig. 2. Same as Fig. 1, but for anthropogenic hydrocarbons (left panels) and biogenic hydrocarbons (right panels).

China and the Eastern US, respectively. The hydrocarbon (HC) emissions in the Eastern US represent 12% in case of HC_a and 3.0% in the case of HC_b of the global emissions. By contrast, they are very small in Eastern China (HC_a accounts for 3.7% and HC_b for 2.0% of the global emissions). The relatively small anthropogenic emission of HC is probably due to the fact that fossil fuel sources in China are dominated by coal burning rather than oil (IEA, 2004). The biogenic emissions of HC are particularly low in Northern China where the vegetation density is small. Most of the biogenic (HC_b) emissions are located in Southern China, where the vegetation density is considerably higher (see Fig. 2).

3. Results

3.1. Aerosol characterization of the two regions

Fig. 3 shows the aerosol column density observed by MODIS in the case of fine ($<0.5\ \mu\text{m}$) and coarse

modes ($>0.5\ \mu\text{m}$), respectively. As shown for example by the model study of Tie et al. (2005), aerosols in Eastern China are mainly composed of sulfate, black and organic carbon, and to a lesser extent, of dust. In the Eastern US, aerosols are mainly made of sulfate, black carbon, and organic carbon. The size of sulfate, black carbon, and organic carbon particles is usually small, with a mean radius ranging from 0.05 to 0.20 μm (Martin et al., 2003), which can be considered primarily to be fine particles. The size of dust particles is larger, with a mean radius of typically 2–3 μm (Ginoux et al., 2001), which can be considered primarily as coarse particles. It can be inferred from Fig. 3 that the density of fine particles is twice as large in Eastern China as in the Eastern US. This results from the higher usage of coal fuels in this part of Asia. The coarse particles are most abundant in the Inner-Mongolia desert regions, where mineral dust is mobilized. In the coastal areas of China, the concentration of coarse particles is substantially

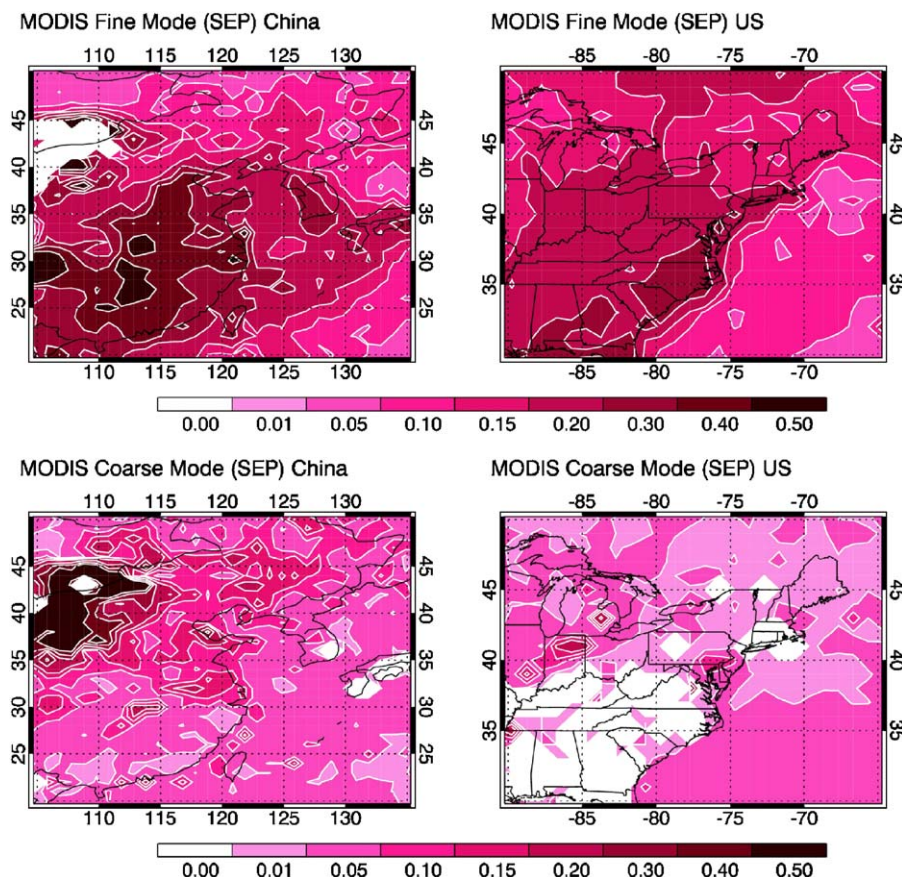


Fig. 3. Measured (MODIS) column aerosols for fine (radius $<0.5\ \mu\text{m}$) and coarse modes (radius $>0.5\ \mu\text{m}$) in Eastern China (left panels) and in the Eastern US (right panels) in September.

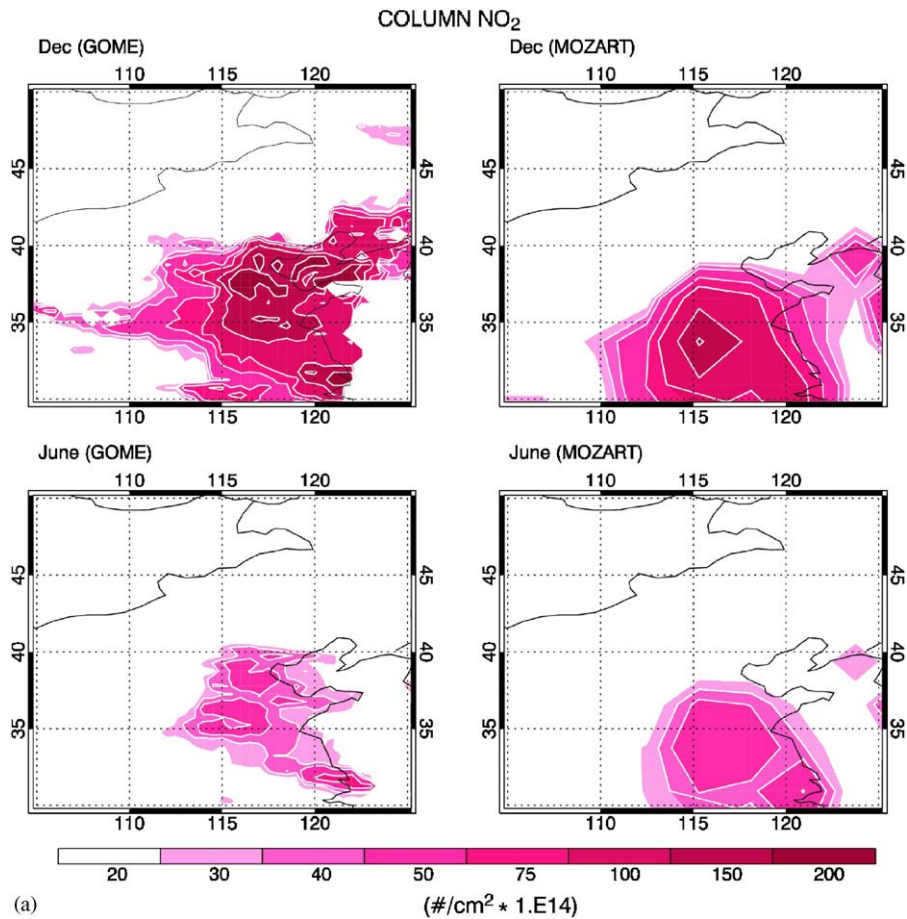


Fig. 4. (a) Measured (GOME, left panels) and calculated (MOZART-2, right panels) column NO₂ (10^{14} #cm⁻²) in June and December for 1997 conditions in Eastern China. (b) Same as Fig. 4a, but for the Eastern US.

lower than in the vicinity of the desert area. There is also an indication that, in the coastal areas of China, the abundance of fine mode particles is higher than that of coarse mode particles, which is consistent with the recent model calculation of Tie et al. (2005). In the Eastern US, the concentrations of coarse particles are very small due to the fact that: (1) the contribution of desert mineral dust is low, and (2) coal burning in this region, which can produce more large particles than oil combustion, is low (IEA, 2004). Both the fine and coarse particle concentrations are high in Eastern China because of high coal fuel usage and intense dust mobilization in this region of the world. The composition of aerosols in Eastern China and the Eastern US is calculated by the MOZART-2 model which includes aerosol modules (Tie et al., 2005). The result shows that in the coast of Eastern

China, sulfate, organic carbon, black carbon, and mineral dust concentrations are approximately 51%, 25%, 20%, and 4% of the total aerosol, respectively. In the west part of Eastern China, sulfate, organic carbon, black carbon, and mineral dust concentrations are approximately 44%, 24%, 10%, and 22% of the total aerosol, respectively. In the coast of the Eastern US, sulfate, organic carbon, black carbon, and seasalt concentrations are approximately 48%, 42%, 8%, and 2% of the total aerosol, respectively. The detailed information is shown in Fig. 16b of Tie et al. (2005). Their study also shows that aerosols affect ozone concentrations throughout the impacts on photolysis rate and the surface reactions of aerosol. For example, the ozone concentrations are reduced in Eastern China by about 10–15% due to the effects of aerosols during summer.

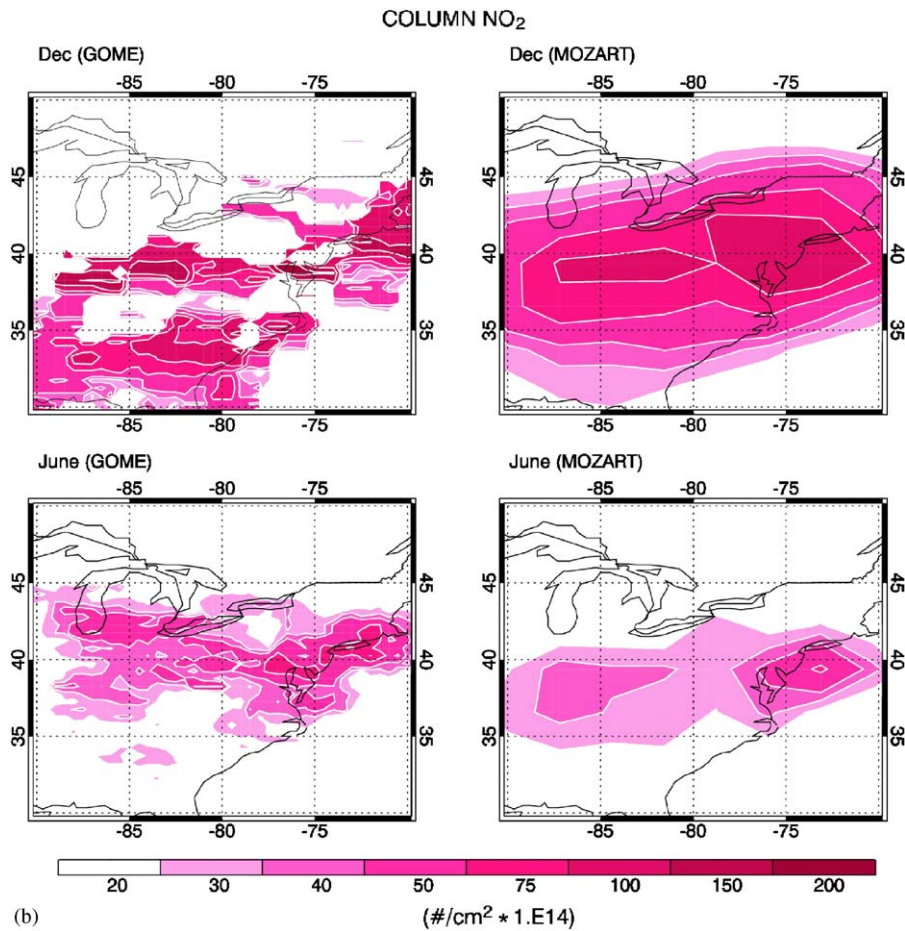
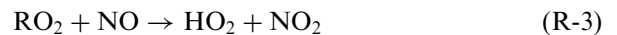
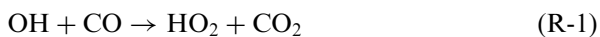


Fig. 4. (Continued)

3.2. Chemical characterization of the two regions

Ozone, which can affect human health and reduce crop production, is produced by the oxidation of chemical precursors, including CH₄, CO and HC in the presence of high atmospheric levels of nitrogen oxides (NO_x = NO + NO₂) and of light. The methane concentration is very uniform in space, and contribution to approximately 10–15% of the ozone photochemical production. Thus, to compare the ozone budgets in the Eastern US and in Eastern China, we will examine the relative contributions provided by the oxidation of carbon monoxide and non-methane hydrocarbons, which are particularly abundant over these polluted regions. A typical chain of reactions is the following:



If the oxidation of OH by CO or HC proceeds slowly, so that small amounts of HO₂ and RO₂ are produced, nitric oxide, rather than reacting with peroxy radicals, reacts with ozone, particularly in the boundary layer where it is emitted (Zhang et al., 2004):



Nitrogen dioxide is further oxidized into nitric acid,



To characterize O₃ in both Eastern China and the Eastern US, information from satellite data on the

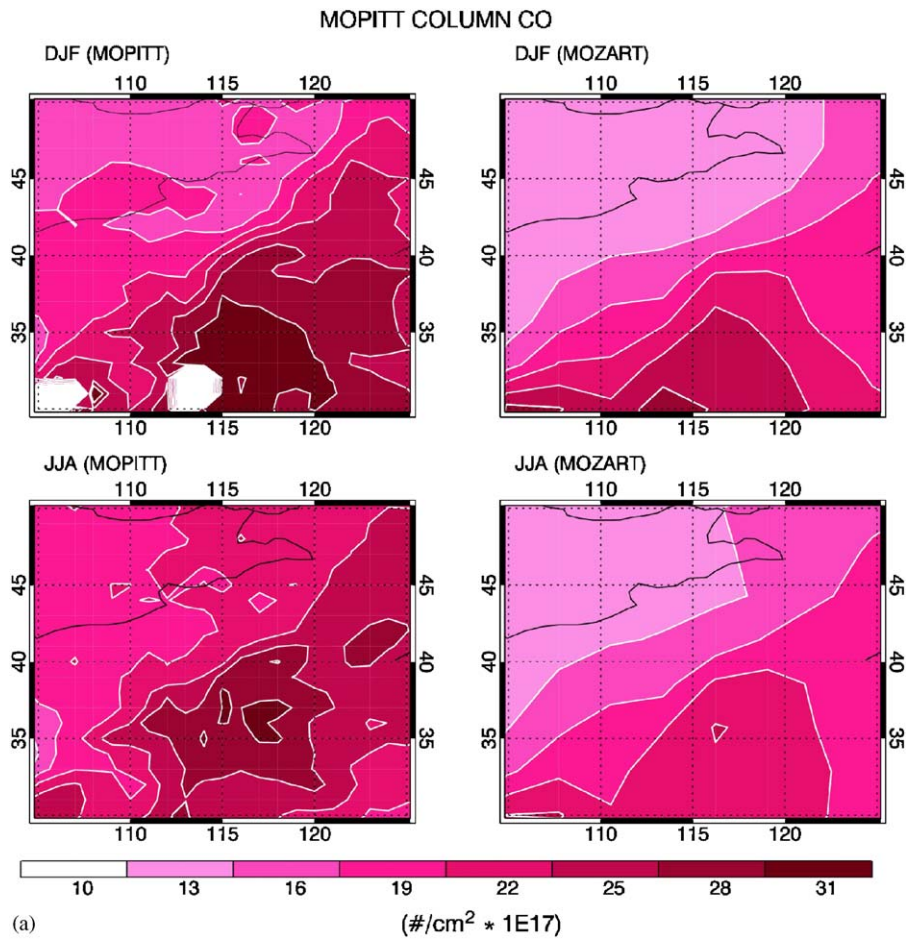


Fig. 5. (a) Measured (MOPITT, left panels) and calculated (MOZART-2, right panels) column CO ($10^{17} \#cm^{-2}$) in summer and winter for 2002–2004 conditions in Eastern China.

NO_2 column (GOME) and on the CO concentration (MOPITT) is useful. However, as satellite observations of hydrocarbons are not available, concentration values need to be estimated from model simulations. The characterizations of hydrocarbons that are available focus primarily on Chinese cities may not be representative of the larger region under condition in the present study. In the case of ozone, calculated rather than measured surface O_3 concentrations will be used in order to ensure consistency in our analysis of the ozone budget.

3.2.1. NO_2 characterization of the two regions

Fig. 4a shows the NO_2 column observed by GOME in June and December 1997 (left panel) and the model calculations for the same period in Eastern China. In both cases, a strong seasonal variability is reported with the highest values occurring in winter when the photochemical lifetime

of NO_2 is largest. There is good consistency between the calculated and measured NO_2 columns. However, the model underestimates the NO_x abundance near the Bo Hai Sea (around $120^\circ E$ and $39^\circ N$), which is probably due to an underestimation of the emissions in this area (see Fig. 1).

In the Eastern US (see Fig. 4b), the magnitudes and seasonal variations of the measured and calculated NO_2 columns are similar. In both cases, a high “band shape” NO_2 pattern is visible between $30^\circ N$ and $45^\circ N$, and is explained by the high surface emissions in this region (see Fig. 1). The strong seasonal variation (high values in winter and low values in summer) is visible in both the measurements and model calculations, but is not explained by the seasonal variation in the NO_x emission since these emissions are about 10% higher in summer than in winter in both regions. We also see that the NO_2 column concentrations (50–150 ($10^{14} \#cm^{-2}$))

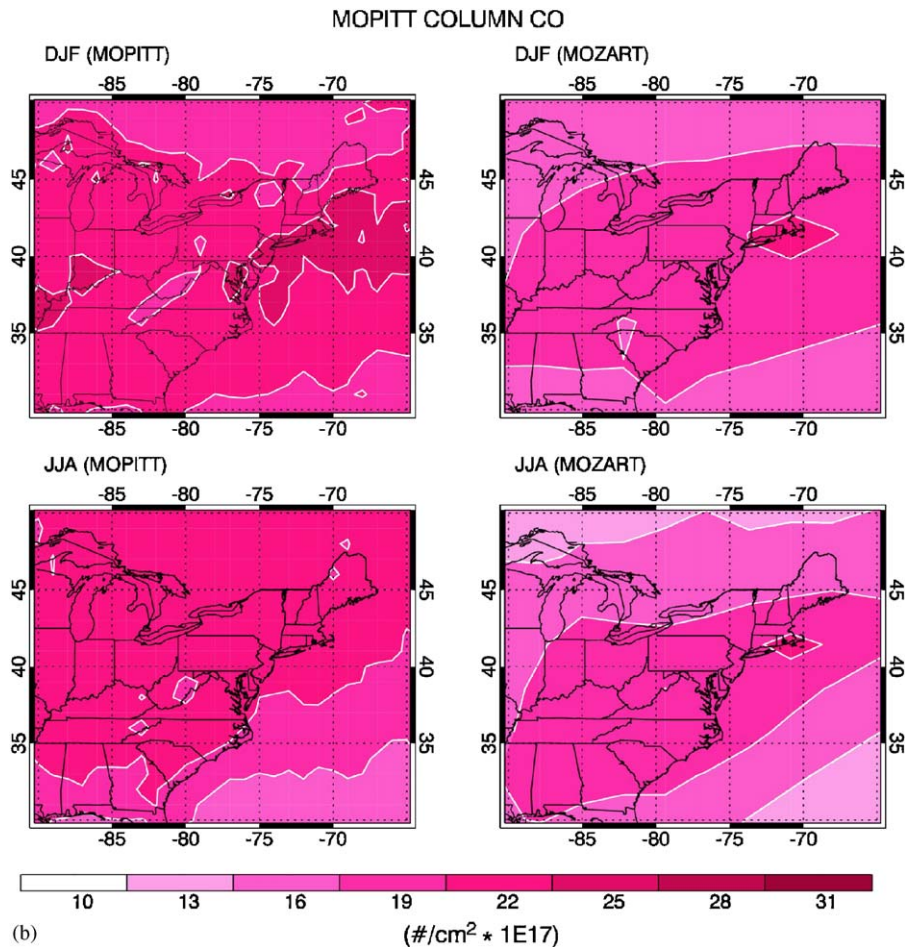


Fig. 5. (Continued)

are high in both the Eastern US and Eastern China when compared to remote regions (e.g., 1–5 (10^{14} #/cm²) in the Pacific region). As mentioned above, the high NO₂ concentrations have important effects on O₃ through reactions (R-1)–(R-7). There is also indication that the spatial distribution of the surface emission is closely related to the calculated column concentrations. This result suggests that the time scale in releasing NO_x from the source is smaller than the time scales of chemical destruction and transport. As a result, the NO_x concentrations are high near the source regions.

3.2.2. CO characterization of the two regions

Fig. 5a shows the CO column density in Eastern China observed by MOPITT (left panel) and calculated by MOZART-2 (right panel) averaged between years 2000 and 2004 for June–July–August (summer) and December–January–February (win-

ter) conditions. The results show that the modeled CO column is underestimated by about 20%. This difference probably results from the fact that the EDGAR database (Olivier et al., 2003) is representative of 1997 conditions (300 Tg year^{-1} CO for industrial emissions) and does not account for the most recent growth in industrial activities and transportation in this region of the world. For example, the energy consumption in China has increased more 300% from 1973 to 2002 (IEA, 2004). The same CO column is shown for the Eastern US in Fig. 5b. Here also, the calculated CO column is somewhat underestimated, which suggests that the EDGAR emissions of CO are also too small in this region. MOZART-2 tends to underestimate the CO concentrations in most regions of the world. The calculated CO concentrations in Eastern China and in the Eastern US are, however, considerably higher than in remote unpolluted areas.

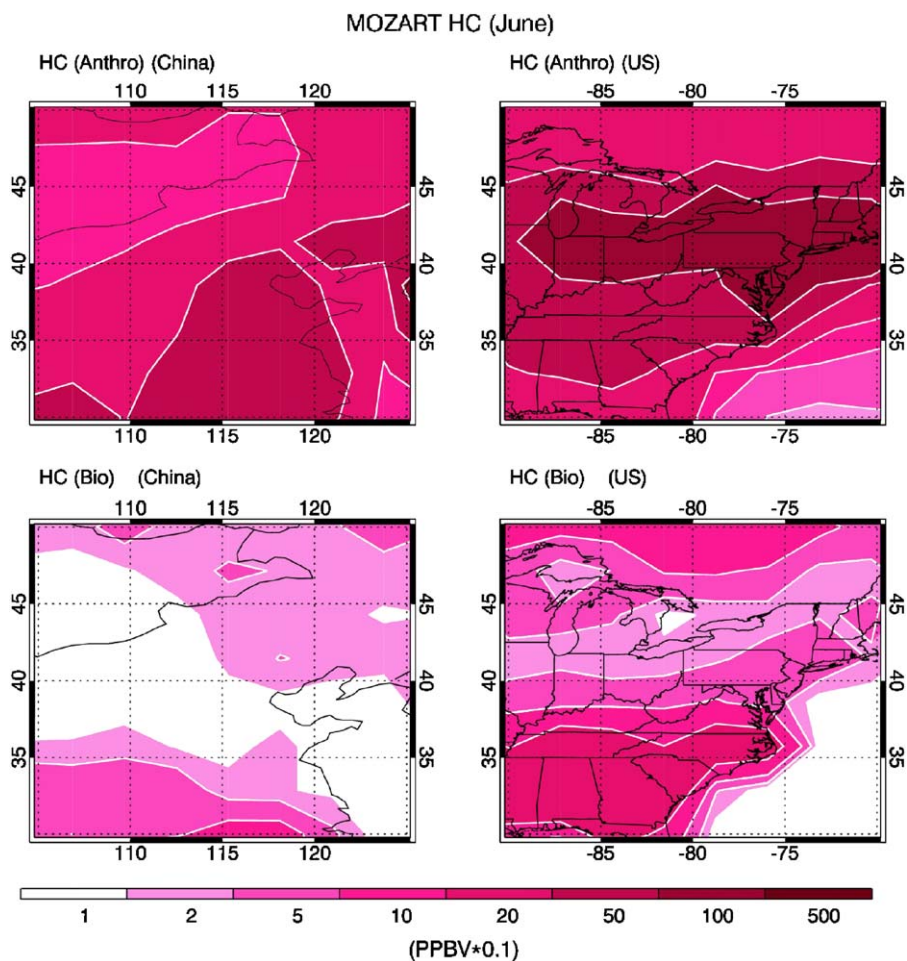


Fig. 6. Calculated surface hydrocarbon concentrations in June. The upper panels are for anthropogenic hydrocarbons (HCA) and the lower panels are for biogenic hydrocarbons (HCB).

3.2.3. HC characterization of the two regions

Currently, satellites do not provide measurements of reactive HCs, and only model results (surface concentrations) are shown in Fig. 6. We separate the HCs according to their origin. The first type HCA is produced by anthropogenic activities and biomass burning, and includes the chemical species in the model (alkanes, alkenes, olefin, and aromatic HCs). The second type HCB results from biogenic emissions, and includes isoprene and terpenes. Fig. 6 shows that the concentration of HCA is much higher in the Eastern US than in Eastern China. For example, between 35°N and 45°N, the abundance of HCA is about two times higher in the Eastern US than in Eastern China. HCB are also more abundant in the Eastern US than in Eastern China. In the middle of Eastern China, the concentrations of HCB are very small due to the lack of vegetation

coverage in this region. Later, we will show that, because of the high chemical reactivity of HCB, the O₃ production from the oxidation of HCB plays an important role in controlling the O₃ concentration in the Eastern US.

3.2.4. Ozone characterization of the two regions

In order to assess the differences between the photochemical characterizations of Eastern China and the Eastern US, we consider in Fig. 7 the surface O₃ concentrations calculated by MOZART-2.

In the Eastern US, the daily averaged O₃ concentrations, as derived by the model, can reach up to 60–70 ppbv during summertime. However, during winter (December), it drops to about 20 ppbv. A strong seasonal variability is also derived for the Eastern China case. However, the summer maximum of O₃ concentrations is lower than in the

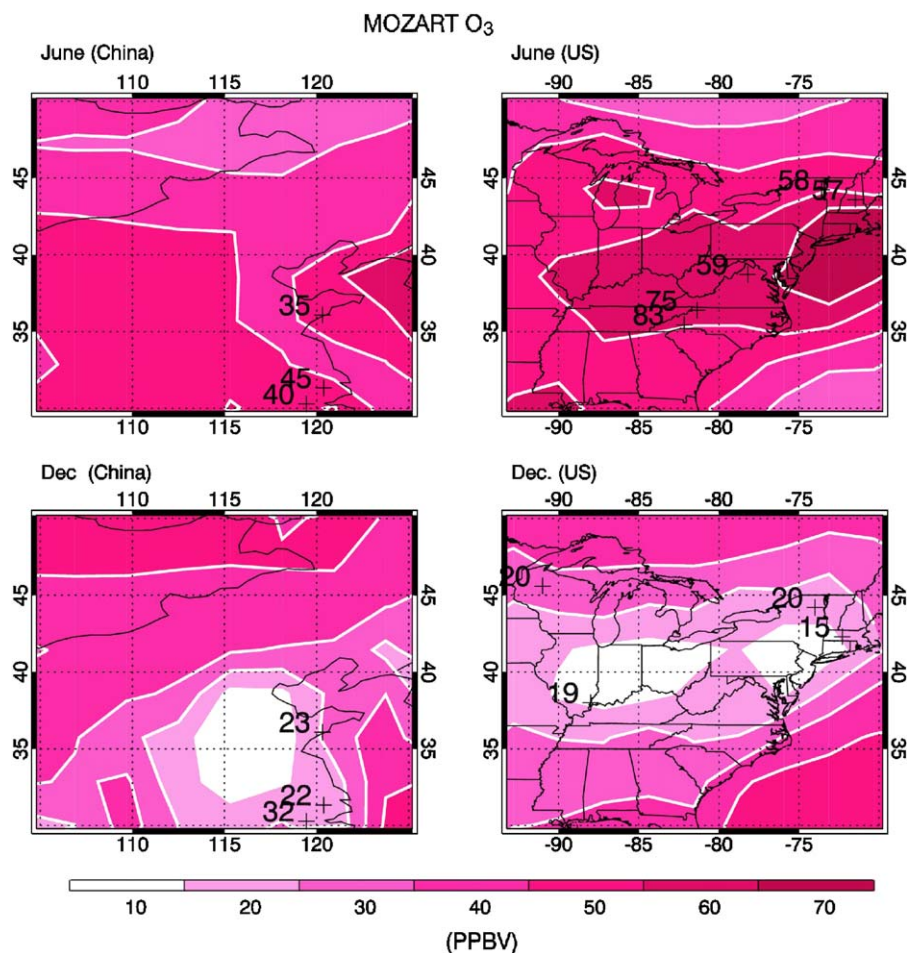


Fig. 7. Same as Fig. 6, except for O₃. The numbers indicate the measured surface ozone (ppbv).

Eastern US (40–50 ppbv compared to 60–70 ppbv). The low winter ozone concentrations are explained in both regions by the rapid titration of O₃ by NO (see Reaction (R-6) and Fig. 4). The calculated surface ozone concentrations are compared to the values measured by Aneja and Li (1992), Logan (1989), Li et al. (1999), and Yan et al., (2003) for several areas in the Eastern US and Eastern China. The monthly mean concentrations provided by these authors are indicated as numbers in Fig. 7, and are also given in Table 2 (along with the uncertainties of the measurements). The measured surface ozone concentrations range from 57 to 83 ppbv in the Eastern US during summer, which is in fair agreement with the model calculations. During winter, the mean surface ozone concentrations in December range from 15 to 20 ppbv. The measured O₃ abundance exhibits also a strong seasonal variation in Eastern

China, with monthly mean values ranging from 35 to 45 ppbv and from 23 to 32 ppbv in June and December, respectively. The comparison between ozone measurements in the two regions suggests that the model captures rather well the seasonal evolution of ozone in both regions. As discussed in Section 4, the lower summertime surface ozone concentrations in Eastern China is probably due to the fact that the summer chemical ozone production is significantly smaller in Eastern China than in the Eastern US. It should be noted, however, that the number of available ozone measurements in China is limited, especially in Central China, so that a detailed analysis of the ozone behavior is not straightforward. More systematic observations are needed, particularly, outside urban area. Other information on the chemical state of the atmosphere in the two regions is given in Table 3.

Table 2
Observed monthly averaged surface ozone over Eastern China and the Eastern US

Site	Location	Sampling date	O ₃ (ppbv)	Ref.
<i>Eastern US</i>				
New York	73.59°W, 44.23°N	June 88	58	1
New Hampshire	71.48°W, 43.59°N	June 88	57	1
Virginia	78.20°W, 38.72°N	June 88	59	1
Virginia	81.36°W, 36.38°N	June 88	75	1
N. Carolina	82.16°W, 35.44°N	June 88	83	1
Indiana	88°W, 38°N	Dec. 77–79	19	2
New York	74°W, 44.2°N	Dec. 73–82	20	2
Massachusetts	72.3°W, 42.3°N	Dec. 77–78	15	2
Wisconsin	91°W, 45.6°N	Dec. 79–81	20	2
<i>Eastern China</i>				
Qindao	120.5°E, 36.1°N	June 95	35	3
Chnshu	119.44°E, 30.28°N	June 2000	45	4
Lin'An	120.38°E, 31.33°N	June 2000	40	4
Qindao	120.5°E, 36.1°N	Dec. 94	23	3
Chnshu	119.44°E, 30.28°N	Dec. 99	22	4
Lin'An	120.38°E, 31.33°N	Dec. 99	32	4

1. Aneja and Li (1992). The uncertainty is $\pm 20\%$ for ozone values greater than 20 ppbv, and ± 4 ppbv for ozone values in the range of 0–20 ppbv.
2. Logan (1989). The uncertainty is approximately $\pm 25\%$.
3. Li et al. (1999). The uncertainty is unknown.
4. Yan et al. (2003). The uncertainty is approximately $\pm 33\%$.

Table 3
Averaged surface chemical concentrations (MOZART-2) and aerosol optical depth (MODIS) in Eastern China and the Eastern US

	E. China	E. US
HCs (anthro)	5 ppb	20 ppb
HCs (bio)	0.1 ppb	2 ppb
CO	200 ppb	200 ppb
NO	2 ppb	2 ppb
NO ₂	10 ppb	15 ppb
OH	0.15 ppt	0.1 ppt
O ₃	40 ppb	70 ppb
Aero (fine)	0.4 (AOD)	0.2 (AOD)
Aero (coarse)	0.1 (AOD)	0.01 (AOD)
High: NO _x , CO, aerosols		High: HC, CO, NO _x
Low: O ₃		High: O ₃
		Low: Aerosols

3.3. Ozone production

From the above analysis, we can infer that the differences in the ozone levels between Eastern

China and the Eastern US could be due to the difference in emission levels of the primary hydrocarbons. To test this hypothesis, we calculate the O₃ production resulting from the major oxidation processes. Under high NO_x concentrations, the ozone production is limited by the hydrocarbon and CO levels, rather than the NO_x concentrations. Thus, the ozone production rate resulting from the oxidation of these compounds can be written as

$$\begin{aligned}
 P[\text{O}_3] &= k_1[\text{OH}][\text{CO}] + \sum_i \{k_{2ai}[\text{OH}][\text{HCa}_i]\} \\
 &\quad + \sum_j \{k_{2bj}[\text{OH}][\text{HCb}_j]\} \\
 &= k_1[\text{OH}][\text{CO}] + k_{2a}[\text{OH}][\text{HCa}] \\
 &\quad + k_{2b}[\text{OH}][\text{HCb}],
 \end{aligned}$$

where k_1 represents the reaction rate constant of OH with CO, and k_{2a} and k_{2b} represent the “effective” reaction rate constants for the reactions of OH with each anthropogenic HC_{a*i*} and each biogenic HC_{b*j*}, respectively. The hypothesis of HC control (rather than NO_x control) of the ozone production is verified when the CH₂O/NO_x concentration ratio is less than 0.28 (Sillman, 1995). Fig. 8 shows that the ratio in both regions is substantially smaller than 0.28.

Fig. 9 indicates that, during summertime (June), the rate of total O₃ production is significantly higher (typically a factor 2) in the Eastern US than in Eastern China. During wintertime (December), the rate of O₃ production decreases rapidly in both regions, and NO titrates ozone rather efficiently.

Fig. 10 shows the contribution to the summertime ozone production resulting from the oxidation of CO, HCa, and HCb, respectively. In Eastern China, the oxidation of CO appears to play a dominant role and represents 54% of the total O₃ production (see Table 4). The oxidation of HCa and HCb accounts for 25% and 21%, respectively. By contrast, in the Eastern US, the oxidation of CO represents only 37% of photochemical production of ozone. The major concentration is provided by the oxidation of HCa and HCb (29% and 34%, respectively). Thus, the oxidation of biogenic hydrocarbons plays important role in the Eastern US. This is consistent with the study by Milne et al. (2000) and that of Chameides et al. (1988), which focuses on the large cities of the Eastern US. Table 3 also shows that the concentrations of CO between the Eastern US and Eastern China are similar, but the HC concentrations in the Eastern US is much higher than Eastern China, suggesting that the absolute contribution of the ozone production

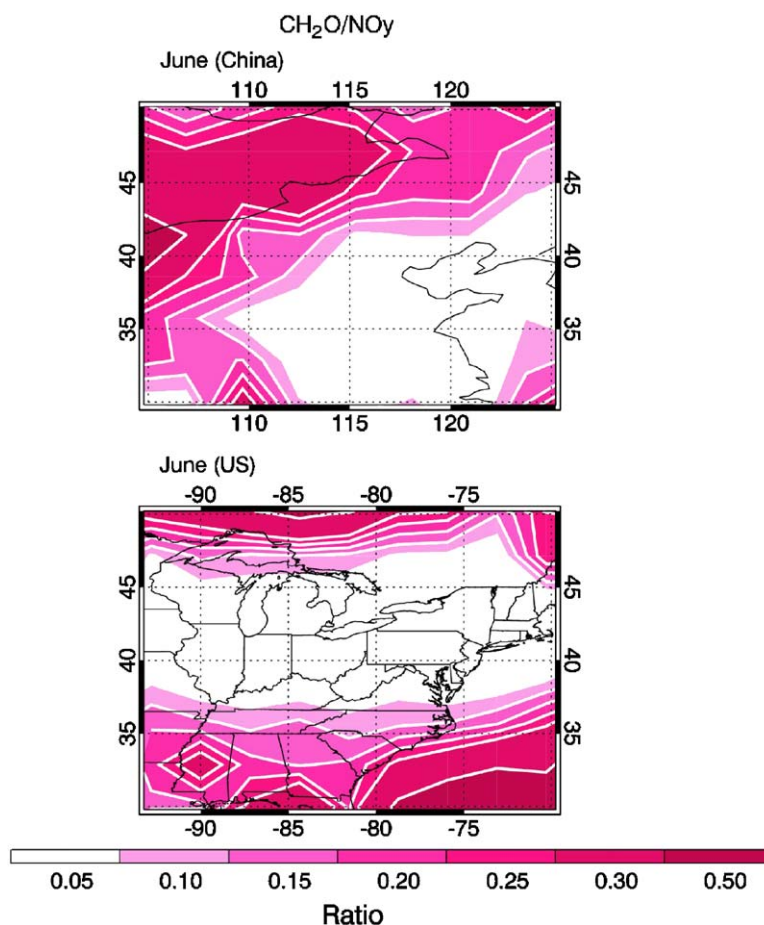


Fig. 8. Calculated $\text{CH}_2\text{O}/\text{NO}_y$ concentration ratio at the surface for June in Eastern China (upper panel) and the Eastern US (lower panel), respectively.

resulted from CO oxidation in Eastern China is comparable to the value in the Eastern US, but the relative contribution is much higher due to the smaller contribution from HC oxidation.

3.4. Potential impact of increase in HCs on ozone in Eastern China

As we described in the previous Sections, the ozone production is largely limited by the lack of HC concentrations in Eastern China. In this section, the impact of the increase in HC emissions in Eastern China on the ozone concentrations is estimated. According to the study of Streets et al. (2003), the anthropogenic NO_x emission will increase about 2.2 times from 1995 to 2020. In our study, we assume that the anthropogenic HC emission will also increase 2.2 times from 1995 to 2020. The purpose of this study is not to quantify

the future ozone concentrations in the Eastern China, rather than to estimate how sensitivity of the ozone concentrations to the increase in HC and NO_x increase in this region.

Fig. 11 shows the calculated surface ozone concentrations due to the increase in anthropogenic NO_x emissions (panel b), due to the increase in anthropogenic HC emissions (panel c), and due to the increase of both HC and NO_x emissions (panel d) in Eastern China in summer (June). The result indicates with the increase in NO_x emissions alone, the surface ozone decreases in Middle Eastern China, because in this region the ozone production is largely limited by the concentrations of HCs (see Fig. 7). By contrast, with increase in anthropogenic emissions of HCs, the surface ozone concentrations significantly increase in Eastern China, indicating that the increase in the emissions of HCs plays an important role for the enhancement in surface

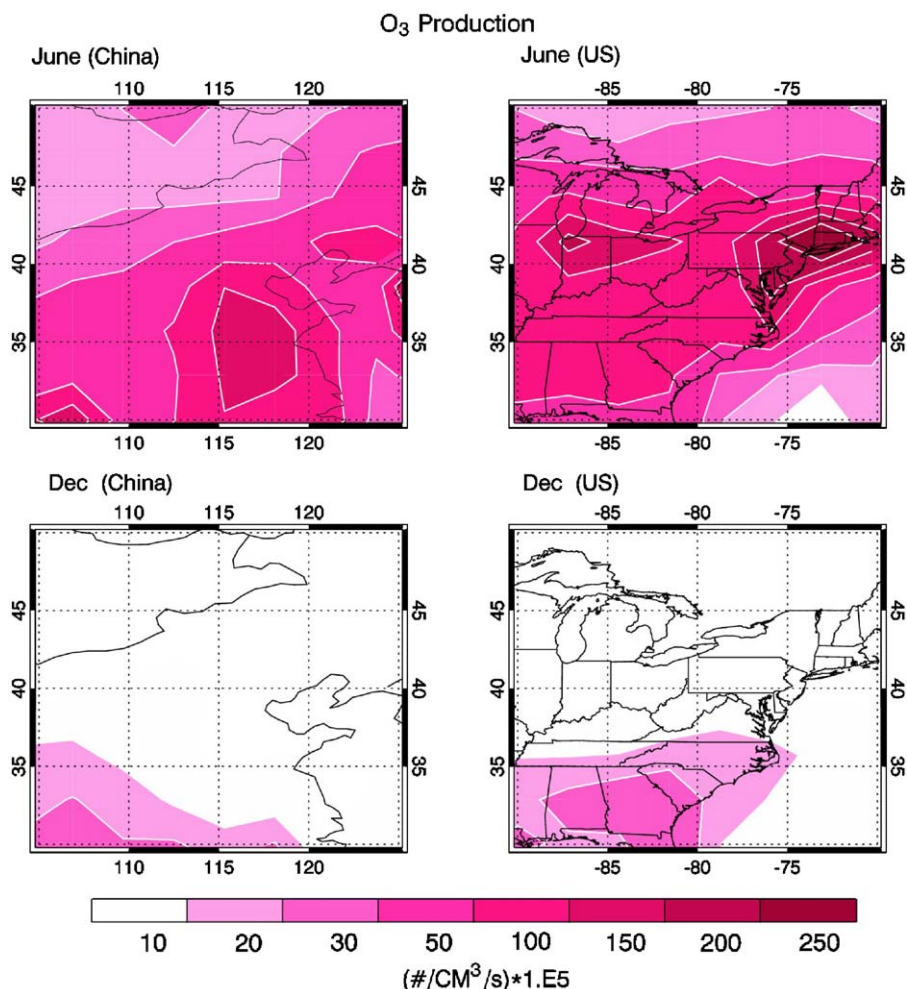


Fig. 9. Calculated total surface O₃ production ($10^5 \# \text{cm}^{-3} \text{s}^{-1}$) in June (upper panels) and in December (lower panels) due to CO and HC oxidations.

ozone in this region. With both the increase in NO_x and HC emissions, the enhancement in the surface ozone concentrations is more evident in this region. The explanation is that with an increase in HC concentrations, the NO_x limited region is enlarged. As a result, the increase in NO_x concentration together with the increase in HC concentration produces more ozone increase. More importantly, the area for the ozone increase is enlarged in this region (see panel d).

4. Summary

In this study, we used satellite observations (MODIS, GOME, and MOPITT), together with a global chemical-transport model of the troposphere

(MOZART-2), to characterize the chemical/aerosol composition over Eastern China and the Eastern US, and to assess the main differences between the photochemical conditions in these two regions. Space observations show that the aerosol optical depth (both fine ($r < 0.5 \mu\text{m}$) and coarse modes ($r > 0.5 \mu\text{m}$)) are substantially higher in Eastern China than the Eastern US. The high aerosol concentrations often lead to severe air pollution problems in Eastern China and, specifically, to reduced visibility. The CO and NO_x concentrations in the two regions are much higher than in “remote” regions such as over the oceans. The high CO and NO_x concentrations are largely due to mobile sources in the Eastern US, and to coal burning in Eastern China. An important difference is that

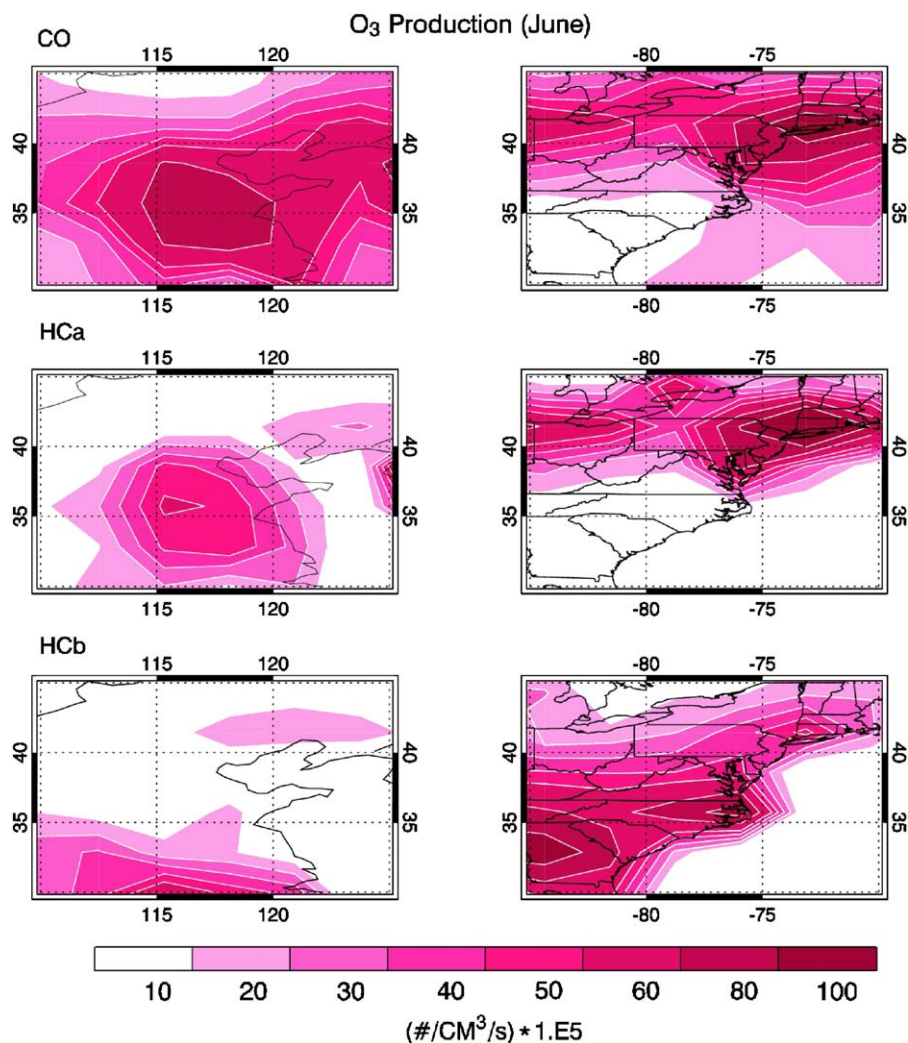


Fig. 10. Calculated total surface O_3 production ($10^5 \# \text{cm}^{-3} \text{s}^{-1}$) due to CO (upper panels), anthropogenic HC (middle panels), and biogenic HC (lower panels) oxidations in June.

non-methane hydrocarbon emissions are considerably lower in Eastern China than in the Eastern US. In China, the biogenic hydrocarbon concentrations are smaller due to limited vegetation coverage (drier climate). In addition, anthropogenic hydrocarbon concentrations are low due to the relatively high usage of coal for energy production. As a result, the rate of ozone production and the O_3 concentrations during summertime are significantly lower in Eastern China (daily averaged values of 40–50 ppbv) than in the Eastern US (daily averaged values of 60–70 ppbv). The analysis also shows that, in Eastern China, the photochemical production of ozone results mainly from CO oxidation (54%), while in the Eastern US, it is largely due to the

Table 4
Percent of total O_3 production due to CO, HCa and HCb in Eastern China and in the Eastern US

	E. China (%)	E. US (%)
CO	54	37
HC (industrial)	25	29
HC (biogenic)	21	34

oxidation of non-methane hydrocarbons (68%). A sensitivity study shows that with increase in anthropogenic emissions of HCs, the surface ozone concentrations will significantly increase in Eastern China. Thus, the increase in the emissions of HCs

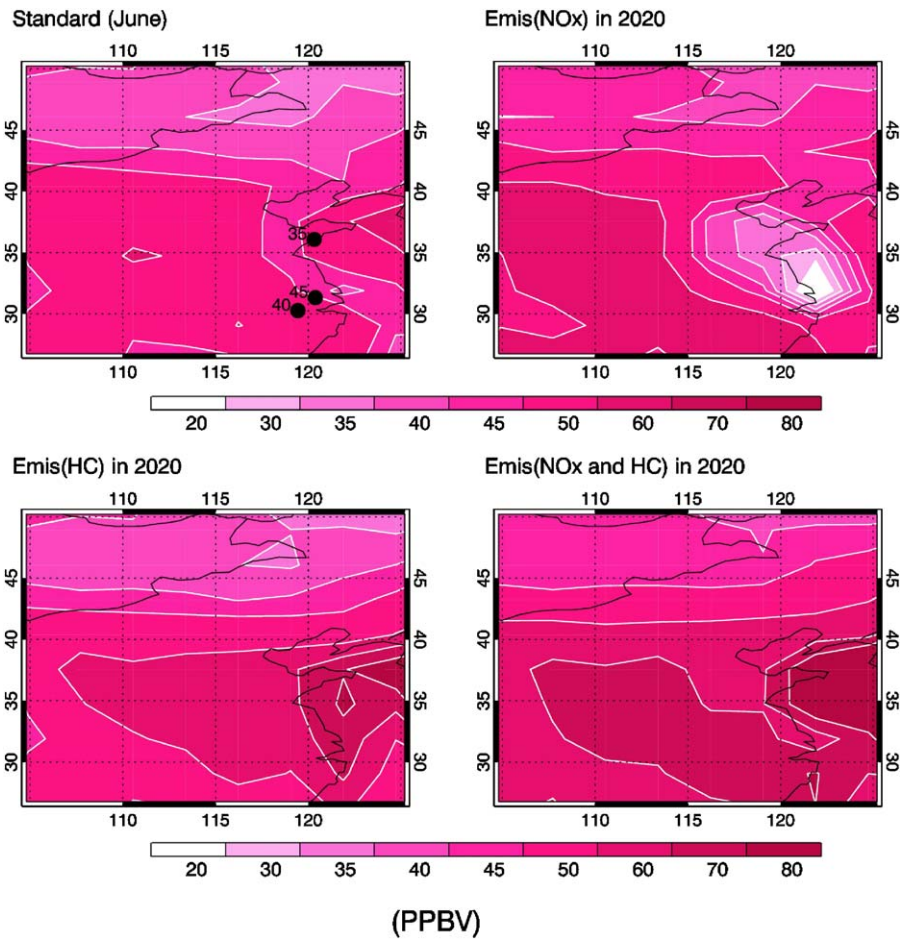


Fig. 11. Calculated surface O_3 concentrations (ppbv) in June by different surface NO and HC emissions: (a) present emissions, (b) Anthropogenic NO emission is multiplied by 2.2, (c) anthropogenic HC emission is multiplied by 2.2, and (d) both anthropogenic HC and NO emissions are multiplied by 2.2.

will play an important role for the enhancement in surface ozone in this region in the future.

Acknowledgments

The authors would like to thank Louisa Emmons and Anne Smith for their valuable suggestions. This research is supported by the National Natural Science Foundation of China (NSFC) under Grant no. 90411009. The National Center for Atmospheric Research is sponsored by the National Science Foundation and operated by UCAR.

References

- Aneja, V.P., Li, Z., 1992. Characterization of ozone at high elevation in the Eastern United States: trends, seasonal variations, and exposure. *Journal of Geophysical Research* 97, 9873–9888.
- Brasseur, G.P., Hauglustaine, D.A., Walter, S., Muller, J.F., Rasch, P., Granier, C., Tie, X., 1998. MOZART: a global three-dimensional chemical-transport-model of the atmosphere. *Journal of Geophysical Research* 103, 28, 265–28,289.
- Burrows, J.P., et al., 1999. The global ozone monitoring experiment (GOME): mission concept and first scientific results. *Journal of the Atmospheric Science* 56, 151–175.
- Chameides, W.L., Lindsay, R.W., Richardson, J., Kiang, C.S., 1988. The role of biogenic hydrocarbons in urban photochemical smog: Atlanta as a case study. *Science* 241, 1473–1475.
- Chu, D.A., Kaufman, Y.J., Zibordi, G., Chern, J.D., Mao, J., Li, C., Holben, B.N., 2003. Global monitoring of air pollution over land from the earth observing system-terra moderate resolution imaging spectroradiometer (MODIS). *Journal of Geophysical Research* 108 (D21), 4661.
- Cunnold, D.M., Steele, L.P., Fraser, P.J., Simmonds, P.G., Prinn, R.G., Weiss, R.F., Porter, L.W., Langenfelds, R.L.,

- Wang, H.J., Emmons, L., Tie, X., Dlugokencky, E.J., 2002. GAGE/AGAGE measurements of methane at 5 sites from 1985 to 1999 and source inferences there from. *Journal of Geophysical Research* 107.
- Deeter, et al., 2003. Operational carbon monoxide retrieval algorithm and selected results for the MOPITT instrument. *Journal of Geophysical Research* 108, 4339.
- Drummond, J.R., 1992. Measurements of pollution in the troposphere (MOPITT). In: Gille, J., Visconti, G. (Eds.), *The Use of EOS for Studies of Atmospheric Physics*. North-Holland, New York, pp. 77–101.
- Friedl, R., 1997. Atmospheric Effects of Subsonic Aircraft: Interim Assessment Report of the Advanced Subsonic Technology Program. NASA Ref. Publ. 2400, 143pp.
- Ginoux, P., Chin, M., Tegen, I., Prospero, J., Holben, B., Dubovik, O., Lin, S.-J., 2001. Sources and distributions of dust aerosols simulated with the GOCART model. *Journal of Geophysical Research* 106, 20225–20273.
- Hauglustaine, D.A., Brasseur, G.P., Walter, S., Rasch, P., Muller, J.F., Emmons, L., Carroll, M.A., 1998. MOZART: a global three-dimensional chemical-transport-model of the atmosphere, 2. Model results and evaluation. *Journal of Geophysical Research* 103, 28,291–28,335.
- Hauglustaine, D.A., Brasseur, G.P., Levine, J.S., 1999. A sensitivity simulation of tropospheric ozone changes due to the 1997 Indonesian fire emissions. *Geophysical Research Letters* 26, 305–3308.
- Hauglustaine, D.A., et al., 2001. On the role of lightning NO_x in the formation of tropospheric ozone plumes: a global model perspective. *Journal of Atmospheric Chemistry* 38, 277–294.
- Horowitz, L.W., Walters, S., Mauzerall, D., Emmons, L., Rasch, P., Granier, C., Tie, X., Lamarque, J.F., Schultz, M., Brasseur, G., 2003. A global simulation of tropospheric ozone and related tracers: description and evaluation of MOZART, version 2. *Journal of Geophysical Research* 108, 4784.
- Huebert, B., Bates, T., Russell, P.B., Shi, G., Kim, Y., Kawamura, K., Carmichael, G., Nakajima, T., 2003. An overview of ACE-Asia: strategies for quantifying the relationships between Asian aerosols and their climatic impacts. *Journal of Geophysical Research* 108.
- IEA, 2004. Key World Energy Statistics. International Energy Agency.
- IPCC, 2001. In: Houghton, J.T., Ding, Y., Griggs, D.J., Noguer, M., van der Linden, P.J., Dai, X., Maskell, K., Johnson, C.J., (Eds.), *Climate Change 2001: The Scientific Basis. Contribution of Working Group I to the Third Assessment Report of the Intergovernmental Panel on Climate Change*. Cambridge University Press, Cambridge, United Kingdom and NY, USA, 881pp.
- Lamarque, J.-F., Hess, P., 2003. Model analysis of the temporal and geographical origin of the CO distribution during the TOPSE campaign. *Journal of Geophysical Research* 108, 8354.
- Lamarque, J.-F., Khattatov, B., Gille, J., Brasseur, G., 1999. Assimilation of MAPS CO in a global three-dimensional model. *Journal of Geophysical Research*, 26,209–26,218.
- Li, X.S., He, Z., Fang, X., Zhou, X.J., 1999. Distribution of surface ozone concentration in the clean areas of China and its possible impact on crop yields. *Advances in Atmospheric Sciences* 16, 154–158.
- Logan, A.J., 1989. Ozone in rural areas of the United States. *Journal of Geophysical Research* 94, 8511–8532.
- Martin, R.V.D., Jacob, D.J., Yantosca, R.M., Chin, M., Ginoux, P., 2003. Global and regional decreases in tropospheric oxidants from photochemical effects of aerosols. *Journal of Geophysical Research* 108 (D3), 4097.
- Mauzerall, D.L., Narita, D., Akimoto, H., Horowitz, L., Walters, S., Hauglustaine, D., Brasseur, G., 2000. Seasonal characteristics of tropospheric ozone production and mixing ratios over East Asia: a global three-dimensional chemical transport model analysis. *Journal of Geophysical Research* 105, 17895–17910.
- Milne, P.J., Prados, A.I., Dickerson, R.R., Doddridge, B.G., Riemer, D.D., Zika, R.G., Merrill, J.T., Moody, J.L., 2000. Nonmethane hydrocarbon mixing ratios in continental outflow air from Eastern North America: export of ozone precursors to Bermuda. *Journal of Geophysical Research* 105 (D8), 9981–9990.
- Olivier, J., Peters, J., Granier, C., Petron, G., Muller, J.F., Wallens, S., 2003. Present and future surface emissions of atmospheric compounds. POET report #2, EU project EVK2-1999-00011.
- Rasch, P.J., Mahowald, N.M., Eaton, B.E., 1997. Representations of transport, convection, and the hydrologic cycle in chemical transport models: implications for the modeling of short-lived and soluble species. *Journal of Geophysical Research* 102, 28127–28138.
- Remer, L.A., et al., 2002. Validation of MODIS aerosol retrieval over ocean. *Geophysical Research Letters* 29 (12), 1618.
- Sillman, S., 1995. The use of NO_x , H_2O_2 , and HNO_3 as indicators for ozone- NO_x -hydrocarbon sensitivity in urban locations. *Journal of Geophysical Research* 100, 14175–14188.
- Streets, D.G., et al., 2003. An inventory of gaseous and primary aerosol emissions in Asia in the year 2000. *Journal of Geophysical Research* 108, 8809.
- Sun, Y., Zhuang, G., Wang, Y., Han, L., Guo, J., Dan, M., Zhang, W., Zhang, Z., Hao, Z., 2004. The air-borne particulate pollution in Beijing: concentration, composition, distribution and sources. *Atmospheric Environment* 38, 5991–6004.
- Tie, X., Brasseur, G., Emmons, L., Horowitz, L., Kinnison, D., 2001a. Effects of aerosols on tropospheric oxidants: a global model study. *Journal of Geophysical Research* 106, 22931–22964.
- Tie, X., Brasseur, G., Zhang, R., Emmons, L., Lei, W., 2001b. Effects of lightning on reactive nitrogen and nitrogen reservoir species in the troposphere. *Journal of Geophysical Research* 106, 3167–3178.
- Tie, X., Zhang, R., Brasseur, G., Lei, W., 2002. Global NO_x production. *Journal of Atmospheric Chemistry* 43, 61–74.
- Tie, X., Guenther, A., Holland, E., 2003a. Biogenic methanol and its impact on tropospheric oxidants. *Geophysical Research Letters* 30, 1881.
- Tie, X., Madronich, S., Walters, S., Rasch, P., Collins, W., 2003b. Effect of clouds on photolysis and oxidants in the troposphere. *Journal of Geophysical Research* 108, 4642.
- Tie, X., et al., 2003c. Effect of sulfate aerosol on tropospheric NO_x and ozone budgets: evidence during TOPSE. *Journal of Geophysical Research* 108, 8364.
- Tie, X., Madronich, S., Walters, S., Edwards, D.P., Ginoux, P., Mahowald, N., Zhang, R.Y., Lou, C., Brasseur, G., 2005.

- Assessment of the global impact of aerosols on tropospheric oxidants, *Journal of Geophysical Research* 110 (D03204), doi:10.1029/2004JD005359.
- WHO, 1998. World Health Organization report.
- Yan, P., Wang, M., Cheng, H., Zhou, X.J., 2003. Distributions and variations of surface ozone in Changshu, Yangtze Delta region. *Acta Metallurgica Sinica* 17, 205–217.
- Zhang, R., Tie, X., Bond, D., 2003. Impacts of anthropogenic and natural NO_x sources over the US on tropospheric chemistry. *Proceedings of National Academic Science* 100, 1505–1509.
- Zhang, R., Lei, W., Tie, X., Hess, P., 2004. Industrial emissions cause extreme diurnal urban ozone variability. *Proceedings of National Academic Science USA* 101, 6346–6350.